

Original Research Paper

Calculating a guaranteed zone of foramen ovale cannulation: a technical note with implications for trigeminal neuralgia

Chad A. Kuhns, D.A.¹, Matthew J. Zdilla, D.C.^{1,2,3*}

¹Department of Natural Sciences and Mathematics, West Liberty University, West Liberty, WV, USA;

²Department of Graduate Health Sciences, West Liberty University, West Liberty, WV, USA;

³Department of Pathology, Anatomy, and Laboratory Medicine (PALM), West Virginia University School of Medicine, Morgantown, WV, USA

Article history

Received: 3 October 2018

Revised: 30 January 2019

Accepted: 31 January 2019

*Corresponding Author:

Dr. Matthew J. Zdilla

West Liberty University
CSC 139; West Liberty, WV,
26074, USA

Email:

mzdilla@westliberty.edu

Abstract: Cannulation of the foramen ovale is often performed for treatment of trigeminal neuralgia. Despite advances in resolution and visualization, fluoroscopy and computed tomography paired with navigation technology have proven unsuccessful in cannulating the foramen. Therefore, approaches to foramen ovale cannulation warrant improvement. This study applies a geometric model to analyze the region of a foramen occupied by a cylindrical surgical tool (e.g., a cannula, stylet, catheter, or needle) inserted at an angle (ϕ) to the plane of the foramen. As the tool passes through the plane of the foramen, its cross-section is an ellipse with a major axis depending on ϕ . Accordingly, the area of the region depends on ϕ , as well as on the radius of the surgical tool. Knowing the area of the region provides a means of comparing a candidate surgical instrument to the foramen it will cannulate when the area of the foramen is known (e.g., as determined from imaging). After accounting for irregularities in the boundary of the foramen, the angle of approach ϕ , and relative orientations of the foramen and the elliptical region occupied by the tool, the geometric model proceeds to describe two new regions: one which guarantees successful cannulation and one which guarantees the tool will not cannulate. The technique predicts when cannulation of a foramen will likely be impossible. Therefore, this method may prevent adverse surgical events and improve the surgical approach and outcomes in the treatment of trigeminal neuralgia.

Keywords: cranial base; neuronavigation; neurosurgery; stereotaxic techniques; trigeminal neuralgia

Introduction

Surgical procedures that require the insertion of a cannula, catheter, stylet, or needle through a bony foramen are commonly performed to gain access to neural structures (Lazorthes and Verdie 1979; Weiser and Seigel 1991; Sindou *et al.* 1997; Janknegt *et al.* 2001; Kanpolat *et al.* 2001; Ong and Keng 2003; Ratto *et al.* 2003; Huntoon 2005; Furman *et al.* 2008; Arishima and Sindou 2010; Messerer *et al.* 2012; Kim *et al.* 2013; Cheng *et al.* 2014; Gitkind *et al.* 2014; Missios *et al.* 2014; Nordenstam *et al.* 2015; Tubbs *et al.* 2015). One of the most commonly cannulated foramina is the foramen ovale of the

sphenoid bone (FO). Cannulation of the FO is performed for electroencephalographic analysis of the temporal lobe among patients undergoing selective amygdalohippocampectomy, (Weiser and Seigel 1991) percutaneous biopsy of parasellar lesions, (Sindou *et al.* 1997; Arishima and Sindou 2010; Messerer *et al.* 2012), administration of opiates into the trigeminal cistern for cancer pain (Esposito and Delitata 1991), occlusion of clival dural arteriovenous fistulas (Urdaneta-Moncada *et al.* 2012), and, most commonly, the treatment of trigeminal neuralgia (TN) (Kanpolat *et al.* 2001; Ong and Keng 2003; Cheng *et al.* 2014; Missios *et al.* 2014).

Trigeminal neuralgia is marked by excruciating neuropathic facial pain so severe it had been formerly dubbed the “suicide disease” (Jiao *et al.* 2018). Though TN is often managed effectively with medications, occasionally surgery is required. Surgeries may include microvascular decompression, gamma knife radiosurgery, or percutaneous procedures, wherein the FO is cannulated. The later procedure may be more appropriate for elderly individuals in whom microvascular decompression is not preferred and among younger individuals whose TN is the result of multiple sclerosis (Kanpolat *et al.* 2000; Berk *et al.* 2003; Ying *et al.* 2017). Moreover, individuals with multiple sclerosis often have TN recurrence and, therefore, may require multiple percutaneous procedures be treated effectively (Martin *et al.* 2015).

Percutaneous transovale cannulation procedures for the treatment of TN such as balloon compression, radiofrequency rhizotomy, and glycerol rhizotomy have been performed by means of a variety of guidance methods (Zdilla *et al.* 2019). For example, fluoroscopy has been commonly utilized for transovale cannulation; however, the radiation required to perform this operation is significant for both the surgeon and patient, having a mean dosage of 1137.18 mGy cm² (range: 639.6 mGy cm² to 1738 mGy cm²) (Fransen 2013). Likewise, fluoroscopy provides poorer visualization of the FO when compared to CT (Georgiopoulos *et al.* 2014). Moreover, a number of reports utilizing fluoroscopic guidance have noted complications due to improper cannulation of the FO (Gökalp *et al.* 1980; Sindou *et al.* 1987; James *et al.* 1995; Göçer *et al.* 1997; Harrigan *et al.* 1998; Ugur *et al.* 2004; Alvernia *et al.* 2010). A number of studies have recently utilized CT in conjunction with navigation systems for the cannulation of the FO (Georgiopoulos *et al.* 2014; Bale *et al.* 2006; Mandat *et al.* 2009; Bohnstedt *et al.* 2012; Van Buyten *et al.* 2009; Lin *et al.* 2011); however, despite improved resolution and visualization of trajectory, even CT paired with navigation technology has proven unsuccessful in cannulating the FO in 5.17% of patients (9:174) because of suspected variation in FO morphology (Georgiopoulos *et al.* 2014).

Several reports have detailed the variation in size and shape of the FO (Berlis *et al.* 1992; Ray *et al.* 2005; Reymond *et al.* 2005; Somesh *et al.* 2011; Daimi *et al.* 2011; Wadhwa *et al.* 2012; Gupta and Rai 2013; Kahairnar and Bhusari 2013; Patil *et al.* 2014; Zdilla *et al.* 2016a; Zdilla *et al.* 2016b; Zdilla

and Fijalkowski 2017). Additionally, approach angles utilized to cannulate the FO have been reported (Pang *et al.* 2012; Yao *et al.* 2013; Huo *et al.* 2013; Huo *et al.* 2014; Zhu *et al.* 2014; Zdilla *et al.* 2016c). However, reports have not taken into account the size and shape of the cross section of the surgical tools that might occupy the planes of these foramina at various angles of approach.

The anatomical diversity of bony foramina has been reported to cause surgical complications (Georgiopoulos *et al.* 2014); however, the interface between foramina and the surgical tools transmitted through the foramina has not been explicitly examined and, therefore, warrants consideration. This report presents a geometric approach by which to analyze the region of a foramen occupied by a surgical instrument (e.g., a cannula, stylet, catheter, or needle) passing through it. Similarly, the report also demonstrates a method to calculate the region of a foramen in which a surgical instrument may pass; if the instrument may pass at all.

Technical Note

Calculating the Area of a Cylindrical Surgical Tool at its Intersection with a Plane

Let r be the radius of the right circular cylindrical cannulating instrument. The intersection of the instrument with the plane of the foramen is an elliptical region (hereafter *cannulation ellipse*), unless the plane is perpendicular to the axis of the cylinder, in which case the intersection is a circular region (Hilbert and Cahn-Vossen 1999). The semi-minor axis of the ellipse (i.e., half its smallest diameter) will be denoted by m and the semi-major axis (i.e., half the greatest diameter) by M . It is clearly the case that $m = r$. The angle ϕ relative to the plane of the foramen at which the instrument is inserted is defined as follows: the axis (center line) of the instrument intersects the plane at a point P , and a vector at P parallel to the axis makes a range of angles with vectors in the plane based at P (Figure 1). The angle ϕ is the smallest of these angles. An alternative and equivalent description of ϕ is as the acute angle between the axis of the cylinder and the orthogonal projection of the axis to the plane of the foramen. In the literature, ϕ is often called the *minimum acute angle*. Using trigonometry it may be shown that $M = \frac{r}{\sin \phi}$. Observe that the minor axis of the ellipse of intersection does not depend of the angle of insertion ϕ . The area of the ellipse is then

given by

$$A = \pi \cdot mM = \frac{\pi r^2}{\sin \phi}$$

As previously stated, when $\phi = 90^\circ$ the ellipse is a circle (Figure 2). In this case, $\sin \phi = 1$ and the area formula becomes $A = \pi r^2$, the formula for the area of a circle of radius r , as expected.

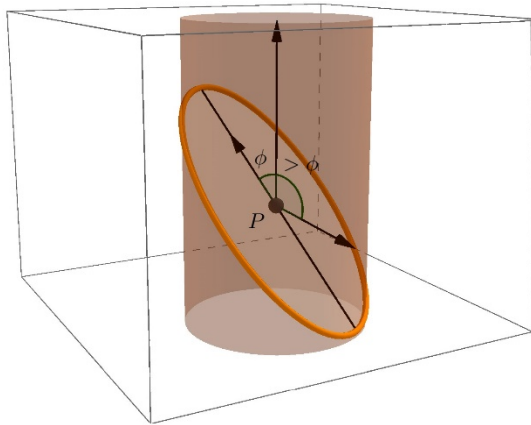


Figure 1. Minimum acute angle between axis of the cylinder (ϕ) (also the trajectory of cannulation indicated by the vertical vector) and the plane. This angle is formed by the axis and the major axis of the ellipse, which is also shown. The minor axis is in the plane of the ellipse and perpendicular to the major axis; it is a diameter of the cylinder.

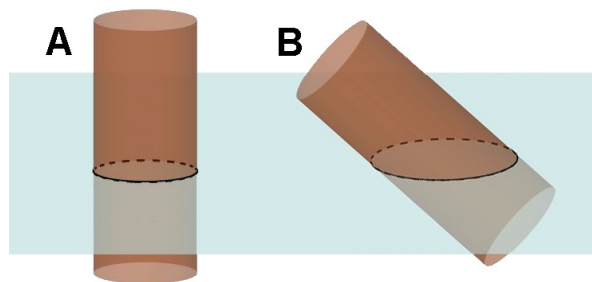


Figure 2. Illustrations demonstrating the intersection of a circular cylinder, representing a cannula, stylet, catheter tube, or needle traversing a plane. **A)** Cylinder (brown) intersecting with a plane (blue) perpendicularly, thereby forming an intersection that is a circle. **B)** Cylinder (brown) intersecting with a plane (blue) obliquely, thereby forming an intersection that is an oval.

Understanding the Relationship between a Cylindrical Surgical Tool and an Elliptical Foramen

With knowledge of the size and shape of an oblique section through a cylindrical surgical tool

(the cannulation ellipse), one can begin to analyze the relationship between the surgical tool and the foramen through which it is intended to cannulate, but only after the size and shape of the foramen is taken into consideration. The FO, for example, is typically described as “oval” in its shape (Berlis *et al.* 1992; Ray *et al.* 2005; Somesh *et al.* 2011; Wadhwa *et al.* 2012; Gupta and Rai 2013; Kahairnar and Bhusari 2013; Patil *et al.* 2014). Occasionally the FO is described as “round” (Ray *et al.* 2005; Somesh *et al.* 2011; Wadhwa *et al.* 2012; Gupta and Rai 2013; Kahairnar and Bhusari 2013; Patil *et al.* 2014). With a view to a precise analysis of the cannulation of the FO by a right circular cylindrical surgical tool, one may make the simplifying assumption that the FO has an elliptical boundary. In the end, this assumption is only slightly restrictive—one may replace the FO boundary with an *inner ellipse*, i.e., an ellipse lying inside the foramen. The obvious choice of inner ellipse is one that is as large as possible. Therefore, understanding when a cylindrical surgical tool will pass through a foramen is reduced to geometry—to the question of exactly when one ellipse (the surgical tool) is completely contained in another (the approximation of the FO).

By using the dimensions of an ellipse bound by the perimeter of a foramen, the diameter r of the surgical tool, and minimum acute angle ϕ of the surgical tool relative to the foramen, and the *offset angle* α between the major axes of the two ellipses, one can calculate a guaranteed cannulation zone (CZ), that is, a region inside the foramen ellipse where the surgical tool will not contact bone. This report is the first to detail such a zone.

The Cannulation Zone

For a given cannulation ellipse and a given foramen ellipse, the CZ is the region given as the set of points inside the foramen ellipse through which the central axis of the surgical tool may pass without the tool leaving the foramen ellipse. Since the foramen ellipse is an inner ellipse, the tool will not contact bone provided the center of the stylet remains within the CZ.

Refer to Figure 3. For clarity, align the ellipse of the foramen so that its major axis is horizontal and define α to be the smaller angle between the major axes of the foramen and cannulation ellipses measured counter-clockwise off of the foramen ellipse. (As mentioned above, the major axis of the

cannulation ellipse is the orthogonal projection of the central axis of the surgical tool to the plane of the foramen.)

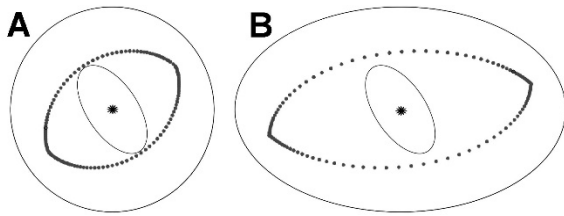


Figure 3. Foramen ovale and cannulating ellipses together with their corresponding cannulation zones encompassed by dotted curves. In **A**) the foramen ellipse is a circle. The cannulating ellipse will not interfere with the foramen ellipse/circle exactly when the center of the cannulating ellipse remains inside this zone. For comparison, in both **A**) and **B**) the same stylet, angle ϕ , and angle α are used.

The key observation that allows one to construct the CZ is that the CZ's boundary points are precisely the centers of cannulation ellipses that are tangent to the foramen ellipse. In other words, the dots on the boundaries of CZs in Figure 3 may be found by translating (without rotating) the cannulation ellipse until it first touches (i.e., is tangent to) the foramen ellipse, and recording the center.

Mathematical Description of the Cannulation Zone

Orient the foramen ellipse so that it is centered at the origin $(0,0)$ and its major axis lies on the x (horizontal) axis. The semi-major and semi-minor axes are, respectively, M and m , and the implicit equation of the ellipse is

$$\frac{x^2}{M^2} + \frac{y^2}{m^2} = 1.$$

The offset angle α is that between the major axes of the foramen and cannulating ellipses as the cannulating instrument passes through the plane of the foramen. The cannulating ellipse is then parameterized by

$$X(t) = \begin{bmatrix} x(t) \\ y(t) \end{bmatrix} = \begin{bmatrix} (M_1 \cos \alpha) \cos t - (m_1 \sin \alpha) \sin t \\ (M_1 \sin \alpha) \cos t + (m_1 \cos \alpha) \sin t \end{bmatrix},$$

where M_1 and m_1 are the semi-major and semi-minor axes of the cannulating ellipse when the axis of the surgical tool is in the center of the foramen ellipse. As mentioned above, boundary points of the CZ may be realized as the centers of a cannulation ellipse that

is tangent to the foramen ellipse (Figure 3).

This observation leads to the following method of finding the CZ:

1. At a point on the cannulation ellipse, compute the slope of its tangent line.
2. Find the point on the foramen ellipse that has a tangent with the same slope.
3. Translate the cannulation ellipse to this point on the foramen ellipse and record the center of the former. This is a boundary point of the CZ.
4. By repeating this process for every point on the cannulation ellipse one obtains all boundary points of the CZ. The CZ itself is then the interior of the region.

Before proceeding to the formulas associated to the aforementioned method, notice that for a given point on the cannulation ellipse there are two points on the foramen ellipse with the same slope. Therefore, one must choose the point on the foramen ellipse so that, when translated, the cannulation ellipse lies *inside* of the foramen ellipse.

We implement this idea by noting that for $t \in [0, 2\pi)$, the tangent vector to the cannulation ellipse is

$$X'(t) = \begin{bmatrix} x'(t) \\ y'(t) \end{bmatrix} = \begin{bmatrix} -(M_1 \cos \alpha) \sin t - (m_1 \sin \alpha) \cos t \\ -(M_1 \sin \alpha) \sin t + (m_1 \cos \alpha) \cos t \end{bmatrix},$$

and its slope is given by

$$S(t) = \frac{dy}{dx} = \frac{dy/dt}{dx/dt} = \frac{-M_1 \sin \alpha \sin t + m_1 \cos \alpha \cos t}{-M_1 \cos \alpha \sin t - m_1 \sin \alpha \cos t},$$

where all derivatives are evaluated at t . From the implicit equation of the ellipse, one computes the slope of the foramen ellipse and then equates the slope to the required $S(t)$:

$$\frac{dy}{dx} = -\frac{x}{y} \cdot \frac{m^2}{M^2} \stackrel{\text{set}}{=} S(t),$$

which has a symmetry: the slope at a point (x, y) on the foramen ellipse is the same at the point $(-x, -y)$; one chooses between these the one for which the center of the cannulation ellipse will lie inside the foramen ellipse.

Solving for y in the last equation and substituting gives

$$1 = \frac{x^2}{M^2} + \frac{\left(-\frac{m^2}{M^2 S} x\right)^2}{m^2} = x^2 \left(\frac{1}{M^2} + \frac{m^2}{M^4 S^2}\right),$$

so that

$$x = \pm \frac{M^2 |\mathcal{S}|}{\sqrt{M^2 S^2 + m^2}}, \quad y = \mp \frac{m^2}{\sqrt{M^2 S^2 + m^2}}$$

where the dependence of \mathcal{S} on t is implied. The required translation of the origin mentioned above is the vector difference of the point on the foramen ellipse and the corresponding point on the cannulation ellipse, and may be computed as $\left(\pm \frac{M^2 |\mathcal{S}|}{\sqrt{M^2 S^2 + m^2}} - (M_1 \cos \alpha) \cos t + (m_1 \sin \alpha) \sin t, \mp \frac{m^2}{\sqrt{M^2 S^2 + m^2}} - (M_1 \sin \alpha) \cos t - (m_1 \cos \alpha) \sin t\right)$,

where the signs must be chosen as described above. All boundary points of the CZ are found by this parameterization.

There are points generated by this method that must be ignored owing to the fact that the stylet ellipse may at the same time be tangent to the foramen ellipse and cross it elsewhere (Figure 4). Disregarding this extraneous data, one sees that the CZ is the fusiform region containing the center of the foramen ellipse.

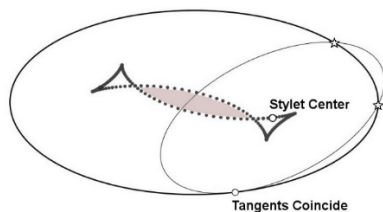


Figure 4. The cannulation zone boundary points generated must be checked for authenticity. This figure illustrates that extraneous cannulation zone boundary points are generated when the cannulation ellipse crosses the foramen ellipse at a distance from a point of tangency; these should be disregarded in practice. The fusiform region located at the center of the image is the true cannulation zone.

Discussion

The contributions of this report are twofold: a methodology for computing the area of the above mentioned region, and a description and derivation of a “cannulation zone” of a foramen on which cannulation is guaranteed to be successful. It is through this zone that the center of the cannulation instrument should be aimed. The analysis of this report is applied to the example of transmitting a

surgical tool through the FO; however, the technical note may be applied to any pairing of surgical tool and foramen.

Understanding the Variables: Examples of Foramen Ovale Cannulation

Variable: Foramen Ovale Area

The FO transmits numerous anatomical structures including the mandibular branch of the trigeminal nerve (V_3), accessory middle meningeal artery, and sometimes the lesser petrosal nerve, emissary veins, and the anterior trunk of the middle meningeal sinus (Dutta 2005; Strandring 2008). In addition to the anatomical variation regarding the contents of the FO, there is also wide variety in the size and shape of the FO, in general (Zdilla *et al.* 2015). A recent study documented that the area contained within the foramen ovale averaged $15.45 \pm 5.09 \text{mm}^2$ with a minimum measurement of 5.58mm^2 and a maximum measurement of 30.50mm^2 (Zdilla *et al.* 2016a).

Variable: Diameter of the Cannula

Numerous reports have documented the use of different gauge cannulae for the treatment of TN. For example, Linderoth and Lind (2012) and Sekimoto *et al.* (2005) utilized 22-gauge lumbar cannulae, whereas Huo *et al.* (2013) and Abdennebi and Guenane (2014) reported using 14-gauge cannulae for percutaneous FO cannulation procedures. A 22-gauge cannula has an outer diameter of approximately 0.7mm, whereas a 14-gauge cannula has an outer diameter of approximately 2.1mm. Reports also note the utilization of a 4 French-gauge Fogarty catheter with an outer diameter of 1.33mm transmitted through the FO (Park *et al.* 2008).

Variable: Cannulation Angle

Prior reports have documented the angles at which the foramen ovale is approached for cannulation (Pang *et al.* 2012; Yao *et al.* 2013; Huo *et al.* 2013; Huo *et al.* 2014; Zhu *et al.* 2014). Pang *et al.* (2012) noted that the angle between the trajectory and the horizontal plane is 49.37 degrees for men and 52.26 degrees for women. The horizontal plane is convenient, in this case, because the perimeter of the FO can be fully

appreciated in axial images. Otherwise, the orientation of the reference plane must be taken into consideration in determining ϕ . For example, Huo *et al.* (2013) described that the angle of introducing the cannula in relation to the Reid line. They noted the cannulation angle ranged from 38.47° - 51.89° with an average of 46.09° (Huo *et al.* 2013). The Reid line deviates from the transverse body plane by approximately 7° to 10° (Ghom 2014). In 2014, Huo *et al.* noted that the angle of introducing the cannula in relation to the Reid line ranged from 38.47° - 51.89° angulation to the Reid line with an average of 46.17° . Likewise, Peris-Celda *et al.* (2013) noted that the needle should form a 45° angle with the hard palate in the lateral radiographic view.

Applying the Technique: Examples of Foramen Ovale Cannulation

Some reports have documented the use of a 22-gauge lumbar cannula to perform retrogasserian rhizolysis for TN (Sekimoto *et al.* 2005; Linderoth and Lind 2012). If an average sized FO (area = 15.45mm^2) were to be cannulated by a 22-gauge lumbar cannula (outer diameter = 0.7mm) at a typical cannulation angle ($\phi = 52.26^\circ$), the area occupied by the cannula in the axial plane (that of the FO) would equal $.64113\text{mm}^2$ and, therefore, the cannula would occupy 4.1% of the foramen. If a small FO (area = 5.58mm^2) were cannulated in the same manner, the cannula would occupy 11.5% of the foramen. The circularity of the oblique section of the lumbar cannula would be 0.97965.

A common cannulation technique uses a 14-gauge cannula that is advanced to the level of the foramen (Park *et al.* 2008; Trojnik and Šmigoc 2012; Xiaochuan *et al.* 2013; Huo *et al.* 2014). After the cannula is advanced to the rim of the FO, a 4 French catheter is advanced into the cranium (Park *et al.* 2008). In this scenario, given a 14-gauge cannula (outer diameter = 2.1mm), a cannulation angle of 52.26° , and a 4 French catheter (outer diameter = 1.33mm), the area occupied by the cannula at the rim of the FO would be 4.38mm^2 (28.3% of average sized FO) and the area occupied by the catheter within the foramen would be 1.76mm^2 .

Visualizing the Technique: Considerations of Foramen Ovale Size

Examples of cannulation zones within foramina

of average, small, and large areas, varied according to the dimensions of a 14-gauge cannula, a 4 French catheter, and a 22-gauge lumbar cannula may be found in Figures 5-7, respectively.

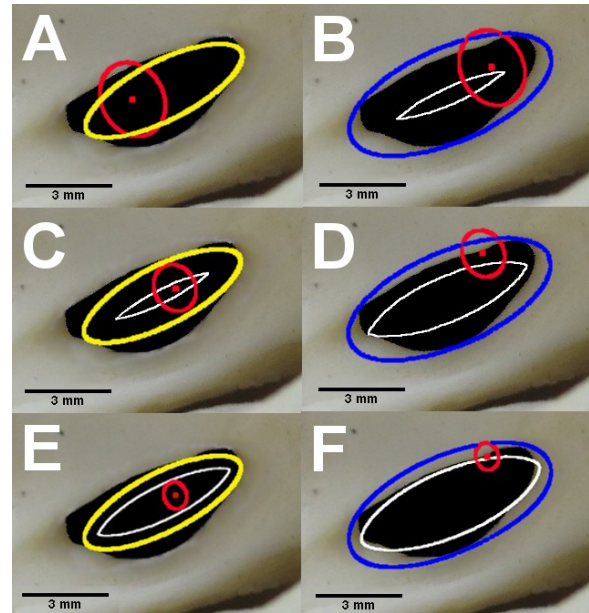


Figure 5. Examples of a foramen ovale of average area (13.8mm^2) with the corresponding cannulation zone computed (accounting for both the orientation of the foramen and that of the surgical instrument) with regard to the dimensions of a 14-gauge cannula, 4 French catheter and again to a 22-gauge lumbar cannula. A 14-gauge cannula is unlikely to pass beyond the level of the foramen, though it may pass through a maximum of 1.6mm^2 (A and B), while the 4 French catheter has at least 1.1mm^2 to at most 6.8mm^2 through which to cannulate (C and D). When cannulated with a 22-gauge lumbar cannula, the cannulation zone area would range from at least 4.6mm^2 to at most 12.0mm^2 (E and F). (WHITE ELLIPSE: cannulation zone; YELLOW ELLIPSE: inner foramen ellipse; BLUE ELLIPSE: outer foramen ellipse; RED ELLIPSE: representation of the surgical tool).

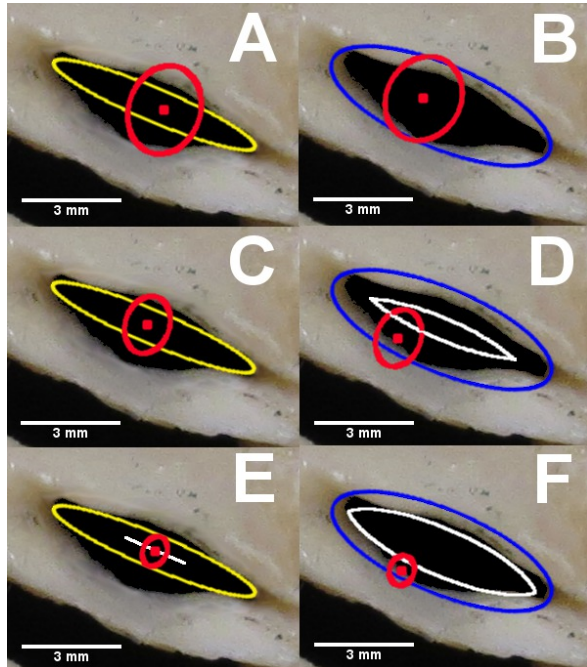


Figure 6. Taking a foramen that is relatively small in area (8.5mm^2) and applying the technique, a 14-gauge cannula is not able to pass beyond the level of the foramen (A and B), while the 4 French catheter may not be able to traverse the foramen (i.e., cannulation zone area of 0.0mm^2) or may be able to traverse foramen within, at most, 3.3mm^2 (C and D). When cannulated with a 22-gauge lumbar cannula, the cannulation zone area would range from at least 0.3mm^2 to at most 7.5mm^2 (E and F). (WHITE ELLIPSE: cannulation zone; YELLOW ELLIPSE: inner foramen ellipse; BLUE ELLIPSE: outer foramen ellipse; RED ELLIPSE: representation of the surgical tool).

As seen in Figures 5-7, some surgical tools are unlikely to pass through the plane of a foramen. In the case of a 14-gauge cannula, a scenario where the cannula is unable to pass through the plane of the foramen is desirable (Figures 5A, 6A, 6B, 6C). In a scenario such as that seen in Figure 6A and 6B, the cannulation of a foramen with a 14-gauge cannula would be impossible; however, in all other scenarios presented in Figures 5-7, cannulation would be possible (and clinically undesirable).

After a 14-gauge cannula is set at the plane of the foramen, in the scenario of the average and large foramen presented here, the 4 French catheter would be guaranteed to traverse the foramen. However, in the case of the small foramen seen in Figure 6A, there is no guaranteed cannulation zone through which the 4 French catheter would pass — a clinically undesirable scenario, and one which may predispose the patient to additional risk with repeated cannulation attempts.

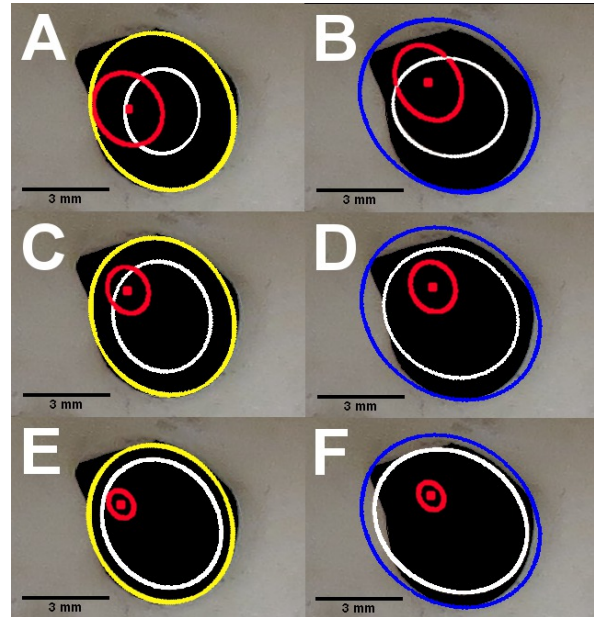


Figure 7. In regard to a particularly large foramen (area= 23.1mm^2), a 14-gauge cannula is able to pass beyond the level of the foramen through an admissible area ranging from at the very least 5.7mm^2 to a maximum of 9.7mm^2 (A and B), while the 4 French catheter has a cannulation zone area ranging from at least 10.0mm^2 to at most 15.3mm^2 (C and D). When cannulated with a 22-gauge lumbar cannula, the cannulation zone area would range from at least 14.3mm^2 to at most 20.4mm^2 (E and F). (WHITE ELLIPSE: cannulation zone; YELLOW ELLIPSE: inner foramen ellipse; BLUE ELLIPSE: outer foramen ellipse; RED ELLIPSE: representation of the surgical tool).

It is worth noting that the 22-gauge lumbar cannula could pass through the foramen in each of the three example scenarios (Figures 5-7). However, Figure 6E demonstrates a guaranteed cannulation zone with an area of a mere 0.3mm^2 — a particularly small target. But, Figure 6E also demonstrates a potential pitfall to this method. When assessing the relationship between the foraminal boundary and the ellipse representing the surgical tool, one can see that the 22-gauge cannula would easily fit through the foramen. The large difference in the fusiform regions seen within the foramen when comparing Figures 6E and 6F help to illustrate the aforementioned point.

Conclusion

Despite improvements in the visualization of trajectory by CT paired with navigation technology cannulation of the foramen ovale may still be unsuccessful in some patients (Georgiopoulos *et al.* 2014). Improper cannulation may lead to potentially serious adverse events. Therefore, further

investigation of the anatomy of the foramen ovale and its relationship with surgical methods and surgical instruments is important.

The mathematical technique described in this report, paired with, for example, CT imaging, may serve as a pre-operative means of determining whether or not a foramen is able to be traversed by a particular surgical instrument. The method also demonstrates the size of the target area through which the surgical instrument may pass; oftentimes, a region significantly smaller than that of the foramen. This methodology should be applied case-by-case; operative methods informed by all other clinically-relevant considerations (e.g., pros and cons of the varied procedures, in general)

Though the clinical utility of this method seems evident in the case of the FO, the method could be translated to any technique in which a circular surgical instrument is to pass through a plane with a defined boundary and orientation.

The method described in this report provides two particularly useful pieces of information: 1) cannulation is guaranteed to fail if the central axis of the stylet is aimed outside of the CZ for an ellipse that *contains* the boundary of the foramen and, 2) cannulation is guaranteed to be successful if the central axis of the stylet is aimed inside of the CZ for an ellipse that is *contained by* the boundary of the foramen. The technique presented in this report will improve foramen ovale cannulation procedures such as those commonly performed to alleviate TN.

Literature Cited

- Abdennebi, B. and L.Guenane. 2014. *Technical considerations and outcome assessment in retrogasserian balloon compression for treatment of trigeminal neuralgia. Series of 901 patients.* Surg. Neurol. Int. **5**:118.
- Alvernia, J.E., M.P. Sindou, N.D. Dang, J.H. Maley, and P. Mertens. 2010. *Percutaneous approach to the foramen ovale: An anatomical study of the extracranial trajectory with the incorrect trajectories to be avoided.* Acta. Neurochir. **152**:1043–1053.
- Arishima, H., and M. Sindou. 2010. *Benefits and pitfalls of percutaneous biopsy for cavernous sinus tumors through the foramen ovale: two case reports.* Minim. Invasive Neurosurg. **53**:194-197.
- Bale, R.J., I. Laimer, A. Martin, A. Schlager, C. Mayr, M. Rieger, B.V. Czermak, P. Kovacs, and G. Widmann. 2006. *Frameless stereotactic cannulation of the foramen ovale for ablative treatment of trigeminal neuralgia.* Neurosurgery. **59**:ONS394-401.
- Berk, C., C. Constantoyannis, and C. Honey. 2003. *The Treatment of Trigeminal Neuralgia in Patients with Multiple Sclerosis using Percutaneous Radiofrequency Rhizotomy.* Can. J. Neurol. Sci. **30**:220-223.
- Berlis, A., R. Putz, and M. Schumacher. 1992. *Direct and CT measurements of canals and foramina of the skull base.* Br. J. Radiol. **65**:653-661.
- Bohnstedt, B.N., R.S. Tubbs, and A.A. Cohen-Gadol. 2012. *The use of intraoperative navigation for percutaneous procedures at the skull base including a difficult-to-access foramen ovale.* Neurosurgery. **70**:177-180.
- Cheng, J.S., D.A. Lim, E.F. Chang, and N.M. Barbaro. 2014. *A review of percutaneous treatments for trigeminal neuralgia.* Neurosurgery. **1**:25-33.
- Daimi, S.R., A.U. Siddiqui, and S.S. Gill. 2011. *Analysis of foramen ovale with special emphasis on pterygoalar bar and pterygoalar foramen.* Folia Morphol. **70**:149-153.
- Dutta, A.K. 2005. *Essentials of Human Anatomy, Head and Neck.* 4th ed. Current Books International. Kolkata.
- Esposito, S., and A. Delitala. 1991. *Transoval administration of opiates into trigeminal cistern for cancer pain. Preliminary report.* Neurochirurgia. **34**:116-118.
- Fransen, P. 2013. *Fluoroscopic exposure during percutaneous balloon compression of the Gasserian ganglion.* J. Neurointerv. Surg. **5**:494-495.
- Furman, M.B., T.S. Lee, A. Mehta, J.I. Simon, and W.G. Cano. 2008. *Contrast flow selectivity during transforaminal lumbosacral epidural steroid injections.* Pain Physician. **11**:855-861.
- Georgiopoulos, M., J. Ellul, E. Chroni, and C. Constantoyannis. 2014. *Minimizing technical failure of percutaneous balloon compression for trigeminal neuralgia using neuronavigation.* I.S.R.N. Neurol. **2014**:630418.
- Gitkind, A.I., T.R. Olson, and S.A. Downie. 2014. *Vertebral artery anatomical variations as they relate to cervical transforaminal epidural steroid injections.* Pain Med. **15**:1109-1114.
- Göçer, A.I., E. Cetinalp, M. Tuna, Y. Gezercan, and F. Ildan. 1997. *Fatal complication of the percutaneous radiofrequency trigeminal rhizotomy.* Acta. Neurochir. **139**:373–374.
- Ghom, A.G. 2014. *Basic oral radiology.* Jaypee Brothers Medical Publishers. New Dheli. p. 139.
- Gökalp, H., Y. Kanpolat, and B. Tumer. 1980. *Carotid-cavernous fistula following percutaneous trigeminal ganglion approach.* Clin. Neurol. Neurosurg. **82**:269–272.
- Gupta, N., and A.L. Rai. 2013. *Foramen ovale – morphometry and its surgical importance.* I.J.M.H.S. **3**:4-6.
- Harrigan, M.R., and W.F. Chandler. 1998. *Abducens nerve palsy after radiofrequency rhizolysis for trigeminal neuralgia: Case report.* Neurosurgery. **43**:623–625.
- Hilbert, D., and S. Cohn-Vossen. 1999. *Geometry and the Imagination.* Chelsea Publishing. New York. pp. 7-11.
- Huntoon, M.A. 2005. *Anatomy of the cervical intervertebral foramina: vulnerable arteries and ischemic neurologic injuries after transforaminal epidural injections.* Pain. **117**:104-111.
- Huo, X., X. Sun, J. Luo, N. Guan, W. Guo, and Z. Zhang. 2013. *Percutaneous microballoon compression for trigeminal neuralgia using Dyna-CT.* Interv. Neuroradiol. **19**:359-364.
- Huo, X., X. Sun, Z. Zhang, W. Guo, N. Guan, and J. Luo. 2014. *Dyna-CT-assisted percutaneous microballoon compression for trigeminal neuralgia.* J. Neurointerv. Surg. **6**:521-526.
- James, E.A., C.C. Kibbler, and S.H. Gillespie. 1995. *Meningitis due to oral streptococci following percutaneous glycerol rhizotomy of the trigeminal ganglion.* J. Infect. **31**:55–57.
- Janknegt, R.A., M.M. Hassouna, S.W. Siegel, R.A. Schmidt, J.B. Gajewski, D.A. Rivas, M.M. Elhilali, D.C. Milam, P.E. van Kerrebroeck, H.E. Dijkema, A.A. Lycklama à Nijeholt, M. Fall, U. Jonas, F. Catanzaro, C.J. Fowler, and K.A. Oleson. 2001. *Long-term effectiveness of sacral nerve stimulation*

- for refractory urge incontinence. *Eur. Urol.* **39**:101-106.
- Jiao, Y., Z. Yan, S. Che, C. Wang, J. Wang, X. Wang, H. Wang, W. Qi, and Y. Feng. 2018. *Improved Microvascular Decompression in Treating Trigeminal Neuralgia: Application of Nest-Shaped Teflon Fibers.* *World Neurosurg.* **110**:1-5.
- Kanpolat, Y., A. Savas, A. Bekar, and C. Berk. 2001. *Percutaneous controlled radiofrequency trigeminal rhizotomy for the treatment of idiopathic trigeminal neuralgia: 25-year experience with 1,600 patients.* *Neurosurgery.* **48**:524-532.
- Kanpolat, Y., C. Berk, A. Savas, and A. Bekar. 2000. *Percutaneous controlled radiofrequency rhizotomy in the management of patients with trigeminal neuralgia due to multiple sclerosis.* *Acta. Neurochir.* **142**:685-689.
- Khairnar, K.B., and P.A. Bhusari. 2013. *An anatomical study on the foramen ovale and the foramen spinosum.* *J. Clin. Diagn. Res.* **7**:427-429.
- Kim, S.H., W.J. Choi, J.H. Suh, S.R. Jeon, C.J. Hwang, W.U. Koh, C. Lee, J.G. Leem, S.C. Lee, and J.W. Shin. 2013. *Effects of transforaminal balloon treatment in patients with lumbar foraminal stenosis: a randomized, controlled, double-blind trial.* *Pain Physician.* **16**:213-224.
- Lazorthes, Y., and J.C. Verdie. 1979. *Radiofrequency coagulation of the petrous ganglion in glossopharyngeal neuralgia.* *Neurosurgery.* **4**:512-516.
- Lin, M.H., M.H. Lee, T.C. Wang, Y.K. Cheng, C.H. Su, C.M. Chang, and J.T. Yang. 2011. *Foramen ovale cannulation guided by intra-operative computed tomography with integrated neuronavigation for the treatment of trigeminal neuralgia.* *Acta. Neurochir.* **153**:1593-1599.
- Linderoth, B., and G. Lind. 2012. *Retrogasserian rhizolysis in trigeminal neuralgia* in Quinones-Hinojosa A., (ed.), *Schmidek and Sweet: Operative Neurosurgical Techniques, Indications, Methods, and Results.* Elsevier Health Sciences. Philadelphia.
- Mandat, T., B. Brozyna, G. Krzymanski, and J.K. Podgorski. 2009. *An image-guided, noninvasive method of cannulation of the foramen ovale for awake, percutaneous radiofrequency rhizotomy.* *J. Neurosurg.* **111**:1223-1225.
- Martin, S., M. Teo, and N. Suttner. 2015. *The effectiveness of percutaneous balloon compression in the treatment of trigeminal neuralgia in patients with multiple sclerosis.* *J. Neurosurg.* **123**:1507-1511.
- Messerer, M., J. Dubourg, G. Saint-Pierre, E. Jouanneau, and M. Sindou. 2012. *Percutaneous biopsy of lesions in the cavernous sinus region through the foramen ovale: diagnostic accuracy and limits in 50 patients.* *J. Neurosurg.* **116**:390-398.
- Missios, S., A.M. Mohammadi, and G.H. Barnett. 2014. *Percutaneous treatments for trigeminal neuralgia.* *Neurosurg. Clin. N. Am.* **25**:751-762.
- Natarajan, M. 2000. *Percutaneous trigeminal balloon compression experience in 40 patients.* *Neurol. India.* **99**:785-786.
- Nordenstam, J., A.M. Boller, and A. Mellgren. 2015. *Sacral Nerve Stimulation in the Treatment of Bowel Disorders.* *Prog. Neurol. Surg.* **29**:200-212.
- Ong, K.S., and S.B. Keng. 2003. *Evaluation of surgical procedures for trigeminal neuralgia.* *Anesth. Prog.* **50**:181-188.
- Pang, J., S. Hou, M. Liu, H. Feng, L. Zu, Y. Guo, Y. Ma, J. Qin, X. Wang, Y. Feng Jr, and K. Cheng. 2012. *Puncture of foramen ovale cranium in computed tomography three-dimensional reconstruction.* *J. Craniofac. Surg.* **23**:1457-1459.
- Park, S.S., M.K. Lee, J.W. Kim, J.Y. Jung, I.S. Kim, C.G. Ghang. 2008. *Percutaneous balloon compression of trigeminal ganglion for the treatment of idiopathic trigeminal neuralgia: experience in 50 patients.* *J. Korean Neurosurg. Soc.* **43**:186-189.
- Patil, G.V., Shishirkumar, D. Apoorva, Thejeswari, J. Sharif, C. Sheshgiri, and N.K. Sushanth. 2014. *Morphometry of the foramen ovale of sphenoid bone in human dry skulls in Kerala.* *I.J.H.S.R.* **4**:90-93.
- Peris-Celda, M., F. Graziano, V. Russo, R.A. Mericle, and A.J. Ulm. 2013. *Foramen ovale puncture, lesioning accuracy, and avoiding complications: microsurgical anatomy study with clinical implications.* *J. Neurosurg.* **119**:1176-1193.
- Ratto, C., U. Morelli, S. Paparo, A. Parello, and G.B. Doglietto. 2003. *Minimally invasive sacral neuromodulation implant technique: modifications to the conventional procedure.* *Dis. Colon Rectum.* **46**:414-417.
- Reymond, J., A. Charuta, and J. Wysocki. 2005. *The morphology and morphometry of the foramina of the greater wing of the human sphenoid bone.* *Folia Morphol.* **64**:188-193.
- Ray, B., N. Gupta, and S. Ghose. 2005. *Anatomic variations of foramen ovale.* *Kathmandu Univ. Med. J.* **3**:64-68.
- Sekimoto, K., S. Koizuka, S. Saito, and F. Goto. 2005. *Thermogangliolysis of the Gasserian ganglion under computed tomography fluoroscopy.* *J. Anesth.* **19**:177-179.
- Sindou, M., J.M. Chavez, G. Saint Pierre, and A. Jouvett. 1997. *Percutaneous biopsy of cavernous sinus tumors through the foramen ovale.* *Neurosurgery.* **40**:106-110.
- Sindou, M., Y. Keravel, B. Abdennebi, and J. Szapiro. 1987. *[Neurosurgical treatment of trigeminal neuralgia. Direct approach of percutaneous method?].* *Neurochirurgie.* **33**:89-111.
- Somesh, M.S., H.B. Sridevi, L.V. Prabhu, M.S. Swamy, A. Krishnamurthy, B.V. Murlimanju, and G.K. Chettiar. 2011. *A morphometric study of foramen ovale.* *Turk. Neurosurg.* **21**:378-383.
- Standring, S. (ed.). 2008. *Gray's Anatomy: The Anatomical Basis of Clinical Practice.* 40th ed. Churchill-Livingstone/Elsevier. New York. p. 529.
- Trojnik, T., and T. Šmigoc. 2012. *Percutaneous trigeminal ganglion balloon compression rhizotomy: experience in 27 patients.* *ScientificWorldJournal.* **2012**:328936.
- Tubbs, R.S., W.R. May Jr., N. Apaydin, M.M. Shoja, G. Shokouhi, M. Loukas, and A.A. Cohen-Gadol. 2009. *Ossification of ligaments near the foramen ovale: an anatomic study with potential clinical significance regarding transcutaneous approaches to the skull base.* *Neurosurgery.* **65**(6 Suppl):60-64.
- Tubbs, R.S., E. Rizk, M.M. Shoja, M. Loukas, N. Barbaro, and R.J. Spinner (eds.). 2015. *Nerves and Nerve Injuries: Vol 2: Pain, Treatment, Injury, Disease and Future Directions.* Academic Press. London.
- Ugur, H.C., A. Savas, A. Elhan, and Y. Kanpolat. 2004. *Unanticipated complication of percutaneous radiofrequency trigeminal rhizotomy: Rhinorrhea: Report of three cases and a cadaver study.* *Neurosurgery.* **54**:1522-1524.
- Urdaneta-Moncada, A., L. Feng, and J. Chen. 2013. *Occlusion of a clival dural arteriovenous fistula using a novel approach through the foramen ovale.* *J. Neurointerv. Surg.* **5**:e46.
- Van Buyten, J.P., I. Smet, and E. Van de Kelft. 2009. *Electromagnetic navigation technology for more precise electrode placement in the foramen ovale: a technical report.* *Neuromodulation.* **12**:244-249.
- Wadhwa, A., M. Sharma, and P. Kaur. 2012. *Anatomic variations of foramen ovale – clinical implications.* *Int. J. Basic and*

- Applied Med. Sci. 2:21-24.
- Wieser, H.G., and A.M. Siegel. 1991. *Analysis of foramen ovale electrode-recorded seizures and correlation with outcome following amygdalohippocampectomy*. *Epilepsia*. **32**:838-850.
- Xiaochuan, H., S. Xiaoyun, L. Junsheng, G. Ning, G. Wenshi, and Z. Zhenxing. 2013. *Percutaneous microballoon compression for trigeminal neuralgia using Dyna-CT*. *Interv. Neuroradiol.* **19**:359-364.
- Yao, J.H., D. Yao, L. Chen, M. Liu, Y.Q. Zhang, and Y.Q. Li. 2013. *Anatomical study of the relatively safe needling angle of minimally invasive treatment for trigeminal neuralgia*. *J. Craniofac. Surg.* **24**:e429-432.
- Ying, X., H. Wang, S. Deng, Y. Chen, J. Zhang, and W. Wu. 2017. *Long-term outcome of percutaneous balloon compression for trigeminal neuralgia patients elder than 80 years: A STROBE-compliant article*. *Medicine (Baltimore)*. **96**:8199.
- Zdilla, M.J., and K.M. Fijalkowski. 2017. *The Shape of the Foramen Ovale: A Visualization Aid for Cannulation Procedures*. *J. Craniofac. Surg.* **28**:548-551.
- Zdilla, M.J., S.A. Hatfield, K.A. McLean, L.M. Cyrus, J.M. Laslo, and H.W. Lambert. 2016a. *Circularity, Solidity, Axes of a Best Fit Ellipse, Aspect Ratio, and Roundness of the Foramen Ovale: A Morphometric Analysis with Neurosurgical Considerations*. *J. Craniofac. Surg.* **27**:222-228.
- Zdilla, M.J., S.A. Hatfield, K.A. McLean, J.M. Laslo, L.M. Cyrus, and H.W. Lambert. 2016b. *Orientation of the Foramen Ovale: An Anatomic Study with Neurosurgical Considerations*. *J. Craniofac. Surg.* **27**:234-237.
- Zdilla, M.J., S.A. Hatfield, and K.R. Mangus. 2016c. *Angular Relationship between the Foramen Ovale and the Trigeminal Impression: Percutaneous Cannulation Trajectories for Trigeminal Neuralgia*. *J. Craniofac. Surg.* **27**:2177-2180.
- Zdilla, M.J., B.K. Ritz, and N.S. Nestor. 2019. *Locating the foramen ovale by using molar and inter-eminence planes: A guide for percutaneous trigeminal neuralgia procedures*. *J. Neurosurg.* DOI: 10.3171/2018.11.JNS182276
- Zhu, H.Y., J.M. Zhao, M. Yang, C.L. Xia, Y.Q. Li, H. Sun, Y.Q. Zhang, and Y. Tian. 2014. *Relative location of foramen ovale, foramen lacerum, and foramen spinosum in Hartel pathway*. *J. Craniofac. Surg.* **25**:1038-1040.